Production of biodiesel from the novel non-edible seed of *Chrysobalanus icaco* using natural heterogeneous catalyst: Modeling and Prediction Using Artificial Neural Network

Okonkwo C. P,[a,*] Ajiwe V.I.E,[a] Obiadi M.C,[a] Okwu M.O [bc] and Ayogu J.I[de*]

a. Department of Pure and Industrial Chemistry, Nnamdi Azikiwe University, Awka, Nigeria.
b. Department of Mechanical Engineering, Federal University of Petroleum Resources, Nigeria.
c. Department of Mechanical and Industrial Engineering, University of Johannesburg, SA.
d. Department of Pure and Industrial Chemistry, University of Nigeria Nsukka, 410001 Nigeria.
e. Department of Chemistry, Faculty of Mathematical and Physical Science, University College London, London WC1E 6BT, United Kingdom.

*Corresponding author: cp.okonkwo@unizik.edu.ng, jude.ayogu@unn.edu.ng

Abstract

Biodiesel has been referred to as a perfect substitute for diesel fuel because of its numerous promising properties. They are renewable, clean, increase energy security, and improve the environment. The seed oil of *Chrysobalanus icaco* was characterised using Gas Chromatography-Mass Spectrophotometer (GCMS) and Fourier Transform Infrared Spectroscopy (FTIR). The heterogeneous solid catalyst of periwinkle shell ash was prepared in 3 forms: raw, calcined and acid-activated. They were characterised using Scanning Electron Microscope (SEM) and FTIR. The results of the SEM analysis revealed the calcined samples to be a better choice because of their larger surface area. The result showed that the oil yield of the used crop was promising for commercial biodiesel production, with *Chrysobalanus icaco* having a yield of 51.90%.

The reusability of the catalyst for continuous reaction runs showed that the yield of biofuel was still high after five cycles: 92.25 - 80.60% for calcined periwinkle shell ash (PSA) catalyst and 89.26 - 78.50% for acid-activated PSA catalyst. The result of the fuel properties of the biodiesel and their blend indicated their suitability for biodiesel production. Methyl ester blends of 20:80 had viscosity that placed them in 2D grade diesel (2.0-4.3mm^2/s), helpful in powering stationary equipment. Other fuel properties, including acid value, pour point, flash point and density, were within the ASTM D6751 limits for biodiesels. Artificial Neural Network (ANN) was used to compare the experimental value to the simulated value using MATLAB 2020. The seed oil of *Chrysobalanus icaco* trans-esterified with methanol using Periwinkle Shell Ash (PSA) catalyst was proven to be a good source of biodiesel.

Graphical abstract

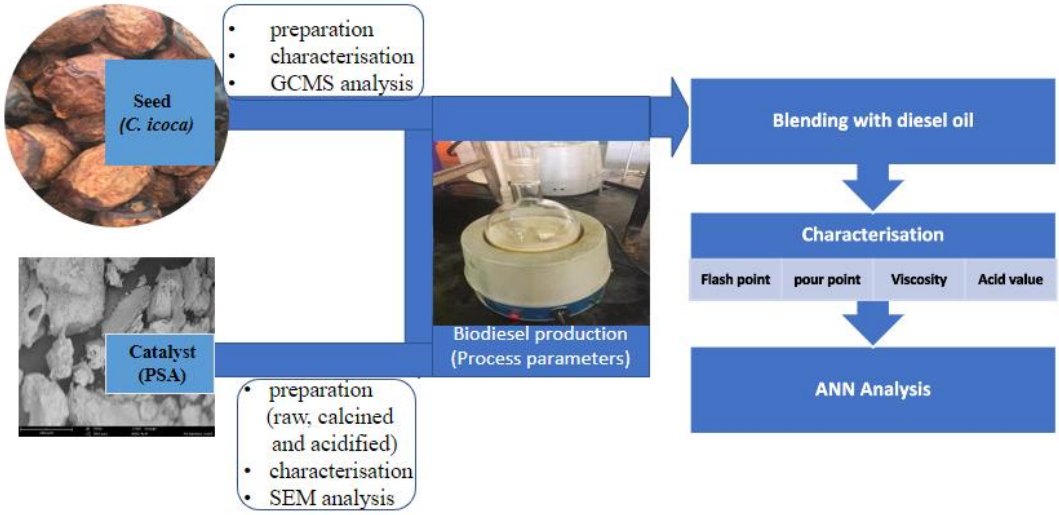

Keywords: *Chrysobalanus icaco*, Catalyst, Trans-esterification, Artificial Neural Network

Highlights:

- Extraction and characterisation of *Chrysobalanus icaco* (*C. icaco*) oil.
- Production of biodiesel from the oil using prepared periwinkle shell ash (PSA) as a heterogeneous catalyst.
- Investigation of the process parameters: catalyst concentration, temperature, time, alcohol ratio, agitation speed and percentage yield.
- Determination of the fuel properties of the biodiesel and diesel blends.
- Comparison of the experimental value with predicted values using an Artificial Neural Network

1. Introduction

The frailty of fossil-based fuels and their negative environmental outcome when utilised in diesel engines has stimulated the hunt for an alternate energy source. Biofuel appears to be a plausible option in this pursuit, as it is renewable and environmentally friendly (Dash & Lingfa, 2018). It consists of monoalkyl esters of long fatty acid chains synthesised from renewable vegetable oils or animal fats, as stipulated by the International Association for Testing and Materials (ASTM). It conforms to the standard of ASTM D6751. The non-recyclability of homogeneous alkali catalysts and waste generation due to subsequent water washing remained one of the industry's significant

drawbacks of the biodiesel production (Gholami *et al.,* 2020). Consequently, efficient and recyclable heterogeneous catalysts made from low-cost materials are a research goal in the biodiesel sector to reduce production costs and waste creation (Ogbu *et al.,* 2018).

Trans-esterification is a chemical process used to produce biodiesel that uses either homogeneous (acid or basic) or heterogeneous (acid, basic, or enzymatic) catalysts. Research has shown that heterogeneous base-catalysed trans-esterification is probably the most popular method because of its fastness and high product yields in short reaction periods (Kara *et al.,* 2019). However, the water content of oils/fats and free fatty acids, the molar ratio of glycerides to alcohol, catalysts, reaction time, and reaction temperature all impact the trans-esterification reaction (Laskar *et al.*, 2018). An acid pretreatment is required to convert the free fatty acid (FFA) to the appropriate methyl/ethyl ester, which is then trans-esterified. The FFA of various feedstock-based triglycerides varies significantly depending on soil, environment and chemical composition (Okonkwo *et al.*, 2021).

Feedstock for biodiesel production can be sourced from vegetable seed oils, waste cooking oil, and animal fats (Verma *et al.,* 2016). Some cheap feedstocks have a significant potential for producing more competitive and sustainable biodiesel because they are high in free fatty acids (FFAs) and moisture (Pikula *et al.,* 2020). Using a standard base-catalysed trans-esterification method creates processing difficulties when converting such feedstock into biodiesel. High FFAs and moisture deactivate base catalysts, resulting in unwanted product (soap) formation and difficulty separating the product, leading to a low biodiesel yield (Ogbu *et al.*, 2018). Cocoplum (*Chrysobalanus icaco*) is a medium-sized shrub endemic to the coast of South America. They are used to cure leucorrhoea, bleeding, and persistent diarrhoea in traditional medicine. They are well-known for their diuretic, hypoglycemic, and anti-antigenic properties. In Northern Brazil, the roots are used to cure diabetes. Several phytochemical investigations on its fruits have revealed the presence of myricetin and pomolic acid. There have also been claims that it has anti-hyperglycemic properties (Feitosa *et al.*, 2012). The leaves have been found to restore insulin sensitivity and blood glucose levels while preventing weight gain in rats fed with a high-fat diet (White *et al.*, 2016). The seed oil included triacylglycerides and a high concentration of unsaturated fats, particularly conjugated linoleic fatty acyls. The presence of palmitic, stearic, oleic, and linoleic acids in the hydrolysate was revealed by GC analysis of the hydrolysed fats (de Aguiar *et al.,* 2017).

An artificial neural network (ANN) is a computational system meant to evaluate and process information in the same manner as the human brain. It is the origin of artificial intelligence (AI), which provides answers to a wide range of issues that have been proven to be difficult or impossible by human or statistical criteria. It is a contemporary computation approach that uses non-linear modelling and complicated datasets. It is critical to link experimental evidence with theoretical truths in various disciplines. It is a statistical tool whose modelling formulation style is based on the simulation of the structure and functions of biological neural networks. Every ANN's fundamental building component is an artificial neuron, a simple mathematical model (function) (Bravo-Moncayo *et al.*, 2019, Hamad *et al.*, 2017, Steinbach & Altinsoy, 2019, Babalola *et al.*, 2018). A model of this type includes three basic sets of rules: multiplication, summation, and activation (Maran *et al.*, 2013, Desai *et al.*, 2008). The ability to detect accurately from minute to large data sets, which are relatively cheap with less time consumption, has made ANN more popular. It is adaptable to numerous disciplines like neuroscience, computation analyses, chemical and environmental engineering, engineering design and application (Khudsange & Wasewar, 2017). The inputs are weighted at the entry of the artificial neuron, meaning that each input value is multiplied by the individual weight. The sum function, which sums all weighted inputs and bias, is located in the centre part of the artificial neuron. The total of previously weighted inputs and bias is passed through an activation function, also known as a transfer function, at the exit of an artificial neuron to create a response. The ANN toolbox from MATLAB is an excellent tool for such predictive analysis (Ayoola *et al.*, 2020, Okwu *et al.*, 2019, Ewim *et al.*, 2022).

There have been several reports and reviews on biodiesel production from different feedstocks ranging from vegetable oil, animal fats, waste cooking oil and algae (Verma *et al.*, 2016, Singh *et al.*, 2020, Ghazali *et al.*, 2015). However, the use of edible vegetable oils as biodiesel feedstock has been of concern as its requirement is increasing, competing with the food supply in the long term. Prime importance is given to alternative biodiesel feedstocks like non-conventional seed oils as these oils will not cause a food crisis leading to economic imbalance. Only one report describing the influence of methanol, ethanol and propanol on the quality of biodiesel produced from *icaco* oil has been published (Ramirez, 2021). To the best of our knowledge, there has not been any other report of the use of *Chrysobalanus icaco* as feedstock (Sanjay, 2013, Singh *et al.*, 2020, Ambat *et al.*, 2018, Shahid & Jamal, 2011). Hence, our research focuses on the production and performance

evaluation of biodiesel from *Chrysobalanus icaco* seed oil using a natural heterogeneous catalyst. It will complete the information gap of utilising other feedstocks to diversify feedstock available in our local environment for their bio-fuel property and usability.

2. Materials and Methods

2.1. Materials - All the reagents were obtained from Sigma Aldrich and used without further purification. The flashpoint was recorded with a Pensky Martens flashpoint tester, while the Soxhlet extractor was used to extract the oil from the raw seeds. Calcination was achieved with a Muffle furnace. The TECHNO R175A diesel engine was used to check the biodiesel's burning capacity. A digital density meter (model AP PAAR DMA 35) and a viscometer were used to test the seed oil and ester blends' densities and viscosity. Fourier-transform infrared spectroscopy (FTIR) was used to analyse the catalyst and seed oil functional group. A spectrophotometer (8400SSHIMADZU) and Emission Scanning Electron Microscope (JSM-670IF) were used to check the morphology of the catalyst. GC- MS QP2010 Plus Shimadzu Japan was used to identify the components of the produced ester.

2.2. Sample Collection and Oil Extraction - A sample of cocoplum seed was purchased from a local market in Onitsha, Anambra State, Nigeria. A taxonomist identified the sample to be *Chyrysobalanus icaco.* The raw sample of Chyrysobalanus icaco was sun-dried before being crushed in an industrial blender. It was sieved via a sieve with a mesh size of 80 μm.

2.3. Oil Extraction by Soxhlet Extraction - The dried sample (*Chyrysobalanus icaco seeds*) was weighed into the semi-permeable cotton material in the thimble of a Soxhlet extractor (500 mL). The Soxhlet was connected to a condenser fixed to a round bottom flask containing n-hexane (400 mL). The Soxhlet extraction system was refluxed until all the oil had been removed from the sample. The de-fatted sample was discarded, and the bottom layer was concentrated in *vacuo* to afford the extracted *Chyrysobalanus icaco* oil, whose percentage yield was calculated.

2.4. Catalyst Preparation and Characterisation - The periwinkle shell sample picked from a local restaurant in Uwani, Enugu, Nigeria, was cleaned, dried, and crushed into a fine paste. A sample of the periwinkle shell (5 g) was calcined to calcium oxide at 800 ^{0}C for 2 h. Some sample (10 g) of the ground periwinkle shell was acidified with conc. sulphuric acid (10 mL) and rinsed with distilled water (approx. 20 mL) until the pH was 7. The samples were dried in an oven

thoroughly and characterised by SEM and FTIR. The characteristics of the catalyst are shown in Table 3.

2.5. Biodiesel production (trans-esterification) - To the catalyst (0.5 g) in a three-neck reactor (500 mL) for each experiment, was added methanol (300 mL). The mixture was stirred for 10 min until complete dissolution. The oil (50 mL) was then added, and the reaction mixture refluxed 2 h at 70 ^{0}C. The reaction mixture was transferred into a separating funnel and allowed to stand for 12 h to allow for glycerol separation. The layers were separated. The methyl ester (biodiesel) was washed with hot water and transferred into a beaker (250 mL). It was then heated to 105 ^{0}C to eliminate moisture and allowed to cool to room temperature. The process was repeated for the various forms of PSA catalysts (Okonkwo *et al.*, 2021).

2.6. Preparation of Biodiesel Blends - Biodiesel blends with fossil diesel of 20%, 40%, 60%, 80% and 100% coded B_{20}, B_{40}, B_{60}, B_{80} and B_{100}, respectively, were prepared for characterisation studies. Fuel properties studied included acid value, density, flash point, pour point and viscosity at different temperatures.

Figure 1: Various processes in the production of the biodiesel

2.6. Artificial Neural Network (ANN) Model

ANN Model comprises an input, hidden and output layer. The modelling has a high potential to contribute to developing renewable energy systems by accelerating biodiesel research (Satya Lakshmi *et al.*, 2020). The experimental design indicates how to obtain the optimal response (Thiruvengadaravi *et al.*, 2009). ANN determination aims to evaluate the performance of differently prepared samples of the periwinkle shell as catalysts in biodiesel yield in the trans-esterification of *C. icaco* seed oil and formulate a system that relates process variables and biodiesel yield using the ANN modelling technique.

3. Results and Discussion

The results of the physicochemical properties of the extracted seed sample are presented (Table 1). The oil obtained from *Chysobalamus icaco* was light brown, and the crop's percentage oil yield was high for large-scale biodiesel production.

Table 1: Physicochemical Properties of the Extracted Oils from *C.icao*

Properties	***C.icao* seed oil**
Colour	light brown
Yield (%)	51.90
Moisture (%)	3.5
Kinematic viscosity @ 40 ^{o}c (mm^2s^{-1})	24.16
Refractive index @ 29 ^{o}c	1.457
Energy value (kJ/kg)	43729
Acid value (mg KOH/g)	0.9
Saponification (mg KOH/kg)	185
Peroxide value (meq/kg)	0.93

Iodine value (g/100 g of oil)	107
Molecular weight (g/mol)	771.66
Flashpoint (^{o}c)	260
Cloud point (^{0}c)	12
Pour point (^{o}c)	6.00
Fire point (^{o}c)	269
Density (gmL^{-1})	0.9278

The overall properties depicted *C.icao* seed oil as a good source of oil for biodiesel production because most of the values conformed to the ASTM standard for oils used in biodiesel production. The acidic compounds possibly found in biodiesel were from the residual mineral acids from the production process, residual free fatty acids from the hydrolysis or post-hydrolysis process of the esters, and finally, from the oxidation by-products in the form of other organic acids (Berthiaume & Tremblay, 2006). Their acid value was low, indicating that the oil could be processed directly into biodiesel using the base-catalysed trans-esterification method (Thiruvengadaravi *et al.*, 2009). High FFAs in oil deactivate the base catalyst and lead to soap formation with a decrease in biodiesel yield.

The results of iodine value showed 107 for *C. icao* seed oil, indicating that it is a non-drying oil. The greater the iodine content, the more unsaturated the oil, and the faster it oxidises and polymerises. The higher the degree of unsaturation in fatty acids, the more susceptible to lipid peroxidation (rancidity). However, antioxidants can protect lipids against lipid peroxidation. Biodiesel with a high iodine content may polymerise and produce deposits on injector nozzles, piston rings, and piston ring grooves. The polymerisation propensity rises with the degree of unsaturation of the fatty acids (Barabás & Todoruț, 2011). As a result, biodiesel with a high iodine content will be less stable at higher temperatures. The Euro norm for iodine value in biodiesel EN 14214 is 120, while the German standard for DIN 5160 is 115 (Calais & Clark, 2004). The type and ester content of the feedstocks used in biodiesel production significantly impacts the iodine value. Kinematic viscosity directly impacts fuel performance, such as atomisation and combustion quality. The kinematic viscosity of the oil was higher than that of the petrol-diesel due to the fatty acid composition and molecular weight of the oil (Ezekwe & Ajiwe, 2011). The oil's kinematic viscosity was within the ASTM range (Knothe & Steidley, 2018).

GC-MS Chart of the Produced Biodiesel

The chart of the produced biodiesel is presented (Figure 2).

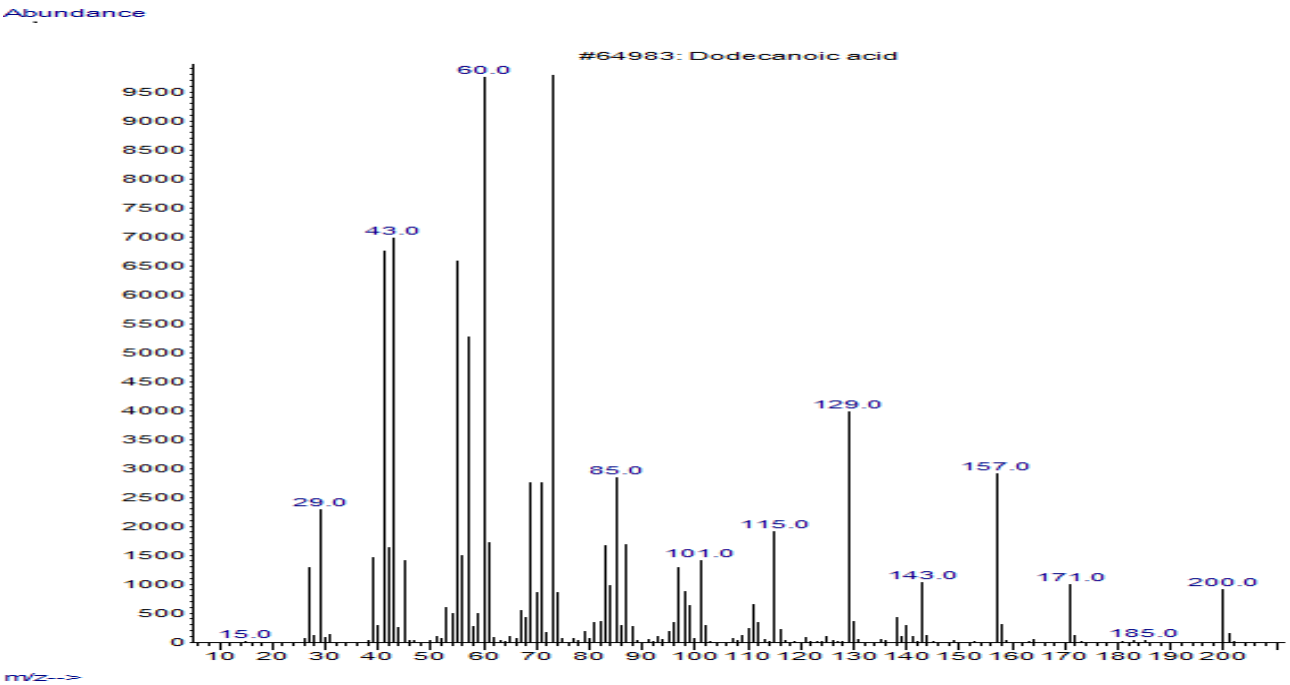

Figure 2: The produced biodiesel chart

Table 2: Fatty acid profile of *C. icao* methyl ester seed oil

S/no	Common name	Systematic name	Short-hand	R. A (%)
1.	Palmitic acid	Hexadecanoic acid	C16:0	6
2	Stearic acid	Octadecanoic acid	C18:0	25
3	Oleic acid	cis-9-octadeaoic acid	C18:1	20
4	Linoleic acid	cis-9,12,15-otacatrienoic acid	C18:3	13
5.	α-parinaric	octadeca-9,11,13,15-tetraenoic acid	C18:2	11
5.	α-licanic	4-oxooctadeca-9,11,13-trienoic acid	C18:3	10
6.	Almonic acid	4-oxo-octadeca-cis-9-trans-11-trans-13-cis-15-tetraenoic acid	C18:4	18
7.	Arachidic acid	5,8,11,14-Eicosatetraenoic acid	C20:1	Trace

Palmitic acid is a natural antioxidant. Table 2 revealed that the principal saturated fatty acids contained in *C.icao* were stearic acid (25%) and palmitic acid (6%), with oleic acid (20%) being the sole unsaturated fatty acid while linolenic acid (13%) was the only polyunsaturated fatty acid. These findings indicated that *C. icao* might have high oxidation stability without the need for additives to promote oxidation stability.

Table 3: Catalysts characterisation of PSA

Parameter	Raw	Acid activated	Calcined
Moisture (%)	0.05	0.06	0.04

Bulk density (g cm^{-3})	0.729	0.571	0.539
pH	6.74	5.73	6.07
Surface Area (m^2 g^{-1})	755	821	856
Carbon (%)	4.08	1.24	2.17
Organic Matter (%)	12.09	3.68	6.44
Loss On Ignition (%)	9.29	3.96	0.85
Particle Density (gcm^{-3})	1.52	1.39	0.83
Total porosity (%)	52.04	58.92	35.06
Ash (%)	3.09	2.44	1.76

3.1. Surface Morphology of the Catalyst

The scanning electron microscope (SEM) was used to elucidate the morphology of the catalysts (Fig 3). The SEM scans showed that the pore widths of the carbon structures in the PSA catalysts increased as the carbonisation period increased and collapsed afterwards. The pores in the calcined catalysts were the most extensive and most ordered. The high pore diameters improved the surface area of the catalyst and favoured bio-oil transformation. For the catalyst made from PSA, partial carbonisation at 800 ^{o}C took longer than 60 min to generate large pore diameters. The biomass conversion might cause the breakdown of the carbon structure after 1 h of carbonisation into graphite (Wang *et al.*, 2014).

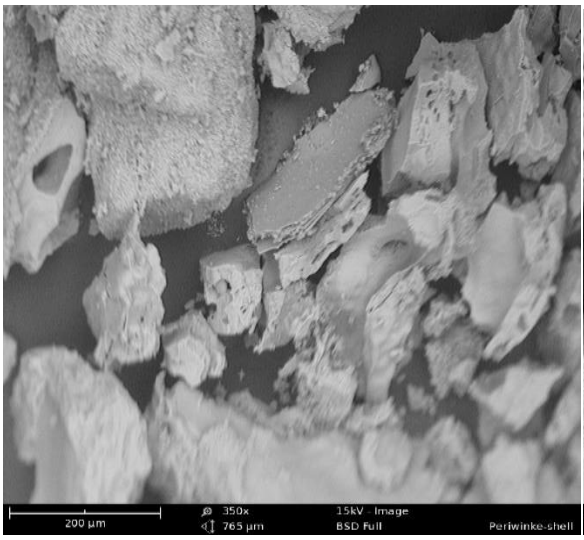

PSA Raw

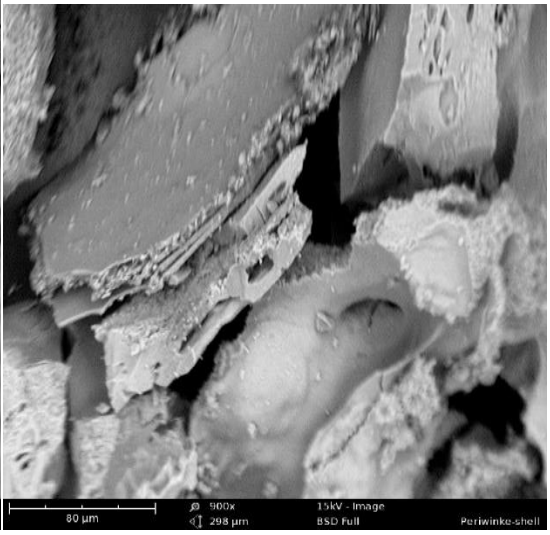

PSA Calcined

PSA Acidified

Figure 3: SEM images of PSA catalyst obtained from the raw, calcined, and acidified form

3.2. Catalyst Reusability

The activity and stability of the catalyst were investigated by reusing it. The samples were calcined and re-acidified after each run. The calcined form was prepared by subjecting the raw PSA to 800 ^{0}C for 2 h. The acidified form was prepared by acidifying the raw PSA (5 g) with Sulphuric acid (5 mL) and rewashed till no trace of acid was detected by testing with litmus paper.

Table 4: Regeneration of PSA Catalyst

Regeneration Runs	The catalyst remains after each run	Yield of CSO (vol. %) (acid-activated)	Yield of CSO (vol. %) (calcined)
1	1.8	89.26	92.25
2	1.3	84.50	87.40
3	0.9	82.80	85.90
4	0.5	80.70	82.10
5	0.2	78.50	80.60

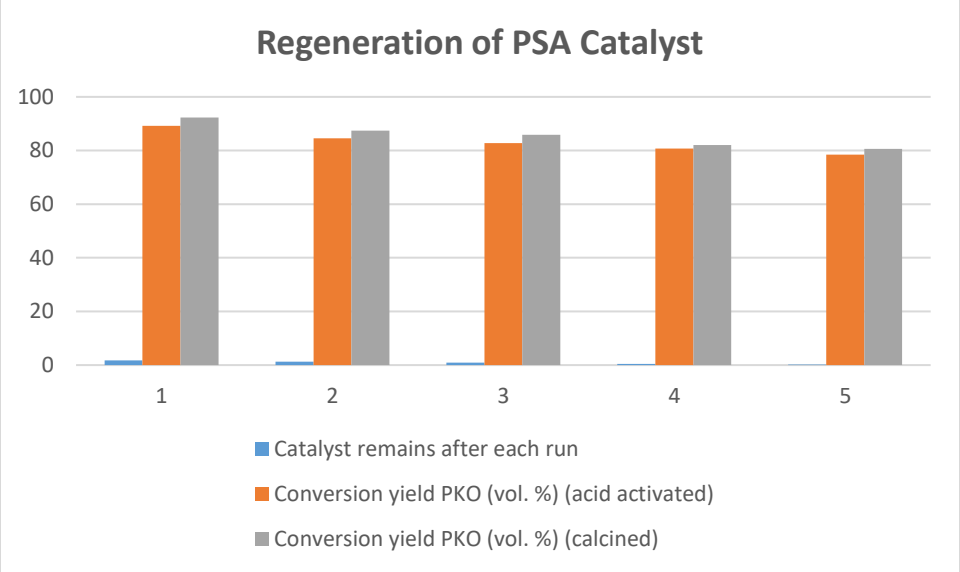

Figure 4: Regeneration of PSA Catalyst

The reusability of the catalyst for subsequent transesterification runs was studied under the same operating conditions after trans-esterification at the optimum operating conditions: methanol: oil (10:1 ratio), catalyst (0.75 g) and 1.5 h reaction time. The initial regeneration run yielded 89.26% and 92.25% for the acid-activated and calcined catalyst for CSO conversion to biodiesel. After the fifth regeneration run, it dropped to 78.50% and 80.60%, respectively, for the catalyst's acid-activated calcined form.

The reusability of the catalyst was evaluated by observing process parameters. The percentage conversion for the calcined (carbon-based) was higher than that of the acid-activated. In the fourth cycle, there seemed to be a decrease in the catalytic activity due to some active sites' deactivation by impurity. It can also be deduced that the leaching of calcium oxide content in the catalyst was the main reason for the sudden drop in conversion.(Kostić *et al.*, 2016, Satya Lakshmi *et al.*, 2020).

Table 5: Fuel Properties of *C. icaco* Seed Oil and its Derivative.

Sample	Density at 28 ºC	Flash point (ºC)	Calorific Value (J/kg)	Pour point (ºC)	Viscosity at 40 ºC (mm^2/s)	Viscosity at 70 ºC (mm^2/s)	Viscosity at 100 ºC (mm^2/s)	Acid value (mgKOH/g)
Diesel	0.8529	76	45179	-8	3.93	2.03	1.43	0.45
C. icaco	0.9278	260	43729	6	24.16	14.06	6.05	1.35
Sample 1	PSA		CALC.		METH.			
B_{100}	0.890	190	44357	6	12. 20	6.08	3.80	1.12
B_{80}	4.0.884	176	44752	4	10.08	4.50	2.40	0.94
B_{60}	0.870	152	44938	2	8.20	3..45	1.95	0.88
B_{40}	0.854	138	44354	-2	6.02	2.78	1.68	0.62
B_{20}	0.844	112	45520	-4	4.20	1.38	0.80	0.32
Sample 2	PSA		ACID		METH.			
B_{100}	0.870	186	44938	4	11.80	5.82	3.20	1.38
B_{80}	0.863	174	45124	3	9.20	4.50	2.42	1.24
B_{60}	0.852	155	45334	2	7.56	3.56	1.87	0.98
B_{40}	0.834	132	45729	1	5.42	2.74	1.06	0.82
B_{20}	0.820	104	45915	-1	5.98	1.96	1.26	0.65
ASTM	0.8-0.9	100	NA	16	1.9-6.0	NA	NA	0.80

NA= not available, min= minimum, max= maximum, PSA= periwinkle shell ash, CALC= calcined, ACID = acidified, METH = methyl ester,

Most samples were within the ASTM range for standard diesel from the result of the blended diesel samples. Sample 1 was produced by trans-esterifying *C. icaco* seed oil with methanol using a calcined PSA catalyst. In contrast, sample 2 was produced by trans-esterifying *C. icaco* seed oil with methanol using an acid-activated PSA catalyst. Their viscosity decreased with continuous blending at a higher temperature.

3.3. Experimental design

The experimental data of the FAME yield for various catalyst amounts, speed of agitation, molar ratio, and temperature are presented (Table 6). The study's dependent variables were % FAME yield, and the independent variables were methanol/oil molar ratio, catalyst quantity, agitation speed, and temperature. The data were input into the ANN toolbox for kinetic simulation of the process with twenty-five experiment samples.

Table 6: Experimental results illustrating the FAME yield from *C. icao* oil using PSA in 3 different forms.

Std Run	A:A	Input variable Catalyst. Conc. % wt of Oil	Exp. Value Yield 1 vol.% (Raw)	Exp. Value Yield 2 (vol.%) (acid activated)	Exp. Value Yield 3 (vol.%) (calcined)
1	23	0.75	51	65	69
2	14	3.75	51	65	69
3	12	0.75	61	65	69
4	30	3.75	61	65	69

5	20	0.75	51	73	69
6	13	3.75	51	73	69
7	5	0.75	61	73	69
8	7	3.75	61	73	69
9	9	0.75	51	65	75
10	2	3.75	51	65	75
11	16	0.75	61	65	75
12	4	3.75	61	65	75
13	18	0.75	51	73	75
14	3	3.75	51	73	75
15	11	0.75	61	73	75
16	26	3.75	61	73	75
17	6	-0.75	56	69	72
18	25	5.25	56	69	72
19	22	2.25	46	69	72
20	24	2.25	66	69	72
21	15	2.25	56	61	72
22	21	2.25	56	77	72
23	29	2.25	56	69	66
24	28	2.25	56	69	78
25	27	2.25	56	69	72
26	10	2.25	56	69	72
27	19	2.25	56	69	72
28	17	2.25	56	69	72
29	8	2.25	56	69	72
30	1	2.25	56	69	72

Table 6 shows the result of biodiesel production obtained using the design expert in MATLAB to simulate the values. The values corresponded to values obtained during the experiment in the laboratory.

The results confirm that the transesterification of vegetable oils using methanol significantly improves their fuel properties (Table 5). The viscosity dropped as the oil was converted to methyl esters from 24.16 - 4.20 mm^2/s for calcined PSA and 5.98 mm^2/s for acidified PSA of the transesterified oil (*C. icaco*). That was within the ASTM range of 1.9 - 6.0 mm^2/s for standard diesel. The reduction in their viscosity is because of replacing heavy alcohol (glycerol) in the oil with simpler alcohol (methanol). High viscosity is a significant drawback in using vegetable oil directly as an alternative fuel in diesel engines(Ajiwe *et al.*, 2006, Jaichandar & Annamalai, 2011). The higher the viscosity, the greater the risk of causing problems (Knothe & Steidley, 2005). The aim of the transesterification of vegetable oils and animal fats for fuel purposes is to reduce their viscosity.

The blending of methyl esters with petroleum diesel improved their viscosity significantly. Methyl esters/diesel (20: 80) of the feedstocks had viscosity that placed them in 2D grade diesel (2.0 - 4.3 mm^2/s) which attributed to their recommendation in the fuelling of mobile equipment while the higher blends fell within 4D grade diesel (5.0 - 34.0 mm^2/s) and could be used for powering stationary equipment (Juliana & Egbulefu, 2015).

The flash points of the feedstocks decreased as they were converted to methyl esters from 260 - 112 ^oC for calcined PSA and 260 -100 ^oC for acidified PSA. The flashpoint is the least temperature at which a fuel will start to vaporise to form an ignitable mixture when it comes in contact with air. It is a safety indicator of fuel. During the transesterification process, the volatile components of the parent oils were reduced. They thus gave a lower yield of the flash point of the fuels—the ASTM specified minimum of 130 ^oC flash point for sole biodiesel. European specifications require at least 101 ^oC, whereas in the US, as low as about 93 ^oC is allowed (Giakoumis & Sarakatsanis, 2019).

The pour point showed that the fuel would not have operational problems during cold weather (as low as 6 ^oC). Other fuel properties of the methyl esters/diesel blends, including acid values and density, were within ASTM D6751 limits. Therefore, the samples could be used as alternative diesel fuels.

The results from the calcined PSA showed a slight disparity in the acidified PSA's acid values (Table 5). Their acid values were on the high side for the acid-activated compared to that of the calcined samples, although the acid values decreased with continuous blending (Ogbu & Ajiwe, 2016).

3.4. ANN Structure

The neural network toolbox used is called from the MATLAB program 2021 version. Levenberg–Marquardt (LM) ANN fitting tool and Logistic Sigmoid Activation Transfer Function 5–15–3 (number of input layer, neurons in hidden layer and output layer nodes) model were implemented using the available experimental data (Fig. 5). Weight parameters were continuously iterated (or refined) to achieve a model with the best possible fit (see Table 7).

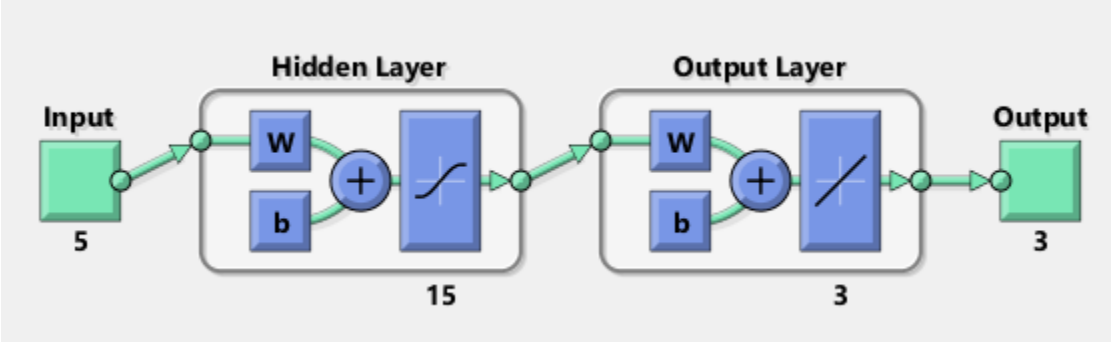

Figure 5: Structure of the ANN Model with Input, Hidden and Output Layer

Table 7: ANN Result for MSE and R-value of the FAME yield for the variables indicated

	Samples	MSE	R
Training	70%	$14.35873e^{-0}$	$8.65794\ e^{-1}$
Validation	15%	$28.52223e^{-0}$	$9.03240\ e^{-1}$
Testing	15%	$8.56118e^{-0}$	$9.46037\ e^{-1}$

Training is the manipulation of input weights (Arulsudar *et al.*, 2005). Data processed by ANN must be classified into two groups. The training set group is used to train the ANN model. The other group, known as the validation and testing set, contains data that differs from the data in the training set. The validation and testing data are used to assess the conformity rate of the trained ANN model. There is no way to describe the relationships and formulas used by ANN once the network has been successfully trained.

The training process is also available in various mechanisms and can be divided into two categories: supervised and unsupervised. The supervised training method divides the dataset into two groups: validation and testing. The conformity rate on the validation dataset is evaluated during the training iterations. Unsupervised training is used for system optimisation, such as reducing energy consumption or increasing profit (Balik *et al.*, 2014). Once the ANN has been trained and tested with the appropriate weights, it can be used to predict the output.

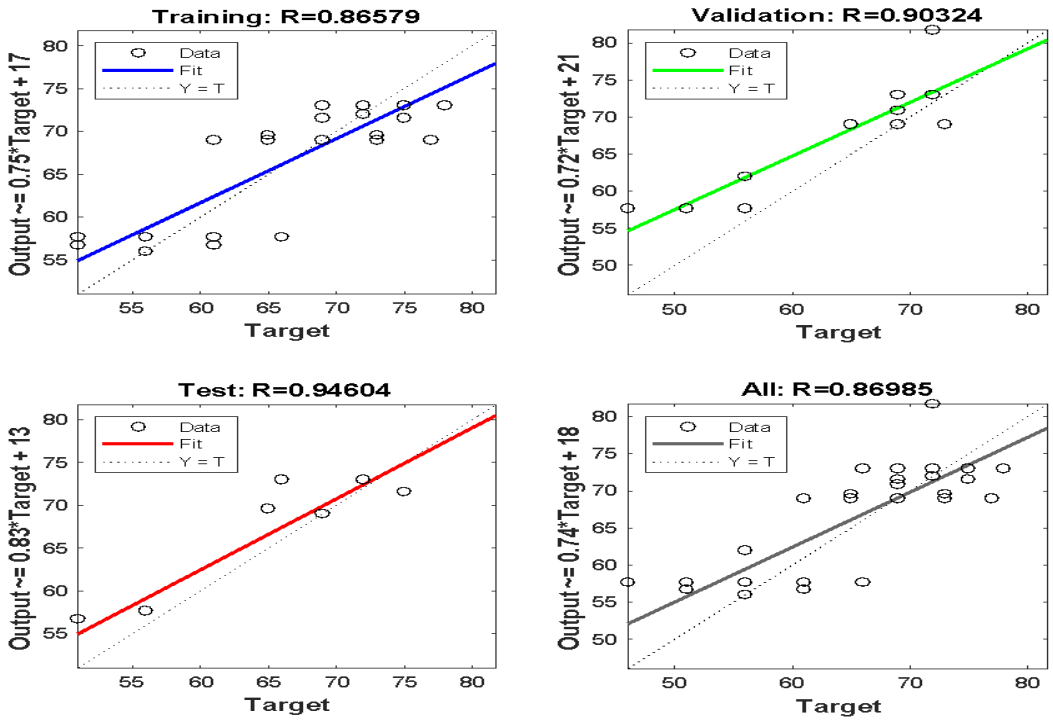

Figure 6: ANN Regression Result for Training, Testing and Validation of Dataset

The R values obtained for training, testing and validation were 0.866, 0.946 and 0.903, respectively. An overall value of 0.86985 was obtained (Fig. 6). The training outcome clearly showed a worthy agreement between the predicted ANN solution model and the result obtained from the experimental yield of biodiesel. The error was significantly minimal. As earlier stated, the satisfactory point is the point where there is a tendency to obtain a perfect connection between determined variables (Krenker *et al.*, 2011). This further means that the solution obtained is satisfactory when the coefficient of determination falls between 0.7 and 1.0. A value of less than 0.7 is considered below the range of acceptable solutions (Okwu *et al.*, 2019).

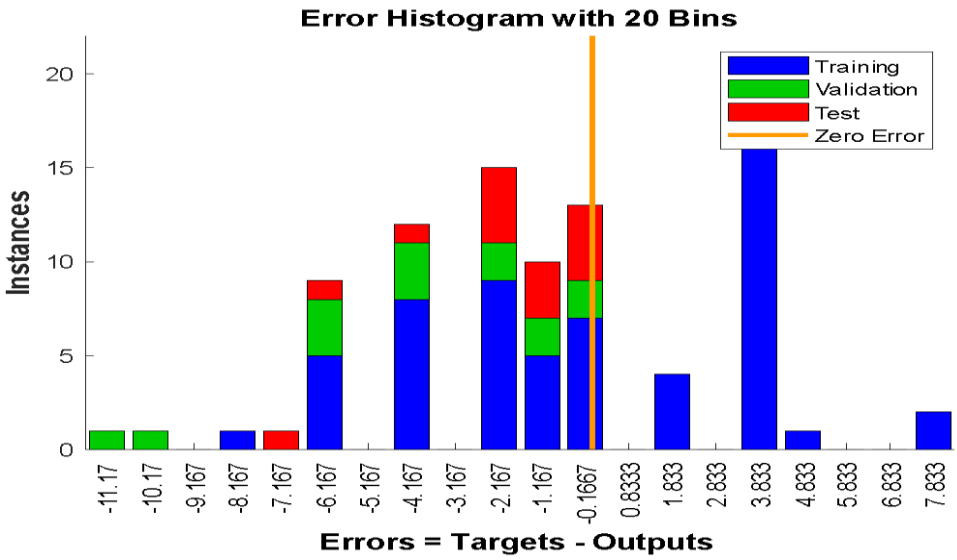

Figure 7: Error histogram of the model

Figure 7 depicts the error histogram for the whole process, highlighting the training, validation, testing, and minimal error. The training set is represented by blue lines, the testing dataset by red lines, and the validation dataset by green text in the error histogram. A thin straight line in the orange text shows the point on the graph when the error tends to zero. Using the back-propagation algorithm method, an error histogram with 20 bins revealed the slightest error of -0.1667 in the study. A perfect validation check was reached at Epoch 3. A satisfactory regression plot was obtained for training, validation, test, and overall plot, using the result generated from the experiment for PSA raw, calcined and acidified catalysts. The satisfactory point is the point where there is a tendency to obtain a perfect connection between determined variables.

Table 8: ANN solution for the predicted values of *C. icao* using the 3 forms of PSA in different forms (raw, acid-activated and calcined)

Std Run	**A:A**	**Input variable Catalyst. Conc. % wt of oil**	**Output value Yield 1 vol.% (Raw)**	**Output Value Yield 2 (vol. %) (acid-activated)**	**Output value Yield 3 (vol.%) (calcined)**	**ANN Predicted value Yield vol.% (Raw)**	**ANN Predicted value Yield (vol. %) (acid-activated)**	**ANN Predicted value Yield (vol.%) (calcined)**
1	9	0.75	57.6666	68.9999	73.0000	57.6666	68.9999	73.0000
2	6	3.75	56.7143	69.5715	71.5714	56.7143	69.5715	71.5714
3	2	0.75	57.6666	68.9999	73.0000	57.6666	68.9999	73.0000
4	14	3.75	56.7143	69.5715	71.5714	56.7143	69.5715	71.5714

5	10	0.75	57.6666	68.9999	73.0000	57.6666	68.9999	73.0000
6	8	3.75	56.7143	69.5715	71.5714	56.7143	69.5715	71.5714
7	4	0.75	57.6666	68.9999	73.0000	57.6666	68.9999	73.0000
8	19	3.75	56.7143	69.5715	71.5714	56.7143	69.5715	71.5714
9	1	0.75	57.6666	68.9999	73.0000	57.6666	68.9999	73.0000
10	13	3.75	56.7143	69.5715	71.5714	56.7143	69.5715	71.5714
11	23	0.75	57.6666	68.9999	73.0000	57.6666	68.9999	73.0000
12	11	3.75	56.7143	69.5715	71.5714	56.7143	69.5715	71.5714
13	12	0.75	57.6666	68.9999	73.0000	57.6666	68.9999	73.0000
14	24	3.75	56.7143	69.5715	71.5714	56.7143	69.5715	71.5714
15	18	0.75	57.6666	68.9999	73.0000	57.6666	68.9999	73.0000
16	3	3.75	57.6667	69.0000	73.0000	57.6667	69.0000	73.0000
17	7	-0.75	57.6667	69.0000	73.0000	57.6667	69.0000	73.0000
18	20	5.25	57.6667	69.0000	73.0000	57.6667	69.0000	73.0000
19	15	2.25	57.6667	69.0000	73.0000	57.6667	69.0000	73.0000
20	5	2.25	57.6667	69.0000	73.0000	7.6667	69.0000	73.0000
21	25	2.25	57.6667	69.0000	73.0000	57.6667	69.0000	73.0000
22	17	2.25	57.6667	69.0000	73.0000	57.6667	69.0000	73.0000
23	21	2.25	57.6667	69.0000	73.0000	57.6667	69.0000	73.0000
24	22	2.25	57.6667	69.0000	73.0000	57.6667	69.0000	73.0000
25	16	2.25	57.6667	69.0000	73.0000	57.6667	69.0000	73.0000

After heedful parametric studies, it became necessary to test the predictive strength of the model techniques using statistical variables such as R - correlation coefficient, R^2 - regression coefficient, root-mean-square error (RMSE) are applied. The equations for computing the above-mentioned statistical variables are presented in systems of Equations 1-5.

$$R = \left(\frac{\sum_{m=1}^{n} (Y_{Pred.m} - y_{Pred})(Y_{exp.m} - y_{exp})}{\sqrt{\sum_{m=1}^{n} (Y_{Pred.m} - y_{Pred})^2 \sum_{m=1}^{n} (Y_{exp.m} - y_{exp})^2}} \right) \quad (1)$$

$$R^2 = 1 - \frac{\sum_{i=1}^{n} (Y_{i,P} - Y_{1,e})^2}{\sum_{i=1}^{n} (Y_{i,P} - Y_{e,ave})^2} \quad (2)$$

$$RMSE = \sqrt{\frac{\sum_{i=1}^{n} (Y_{i,e} - Y_{i,p})^2}{n}} \quad (3)$$

$$\mathrm{MAE} = \sum_{\mathrm{i=1}}^{\mathrm{n}} \frac{\left| (\mathrm{Y_{i,e}} - \mathrm{Y_{i,p}}) \right|}{\mathrm{n}} \quad (4)$$

$$\mathrm{SEP} = \frac{\mathrm{RMSE}}{\mathrm{Y_{e,ave}}} \quad (5)$$

Y_{pred} represents the predicted value of samples, Y_{exp} is the experimental value, Y_i is the observed value of samples, Y_e is the estimated value of samples, and N represents the number of samples. A, B, and C denote independent variables, and β_{ij} is the coefficient of linear terms.

The result obtained from the predicted values in Table 8 showed some similarities with the experimental results (Table 6). This led to the efficacy of using the ANN predictive tool to simulate the production of *C. icaco* using a PSA catalyst in 3 different forms (raw, calcined and acid-activated). Using the statistical indicator showed that the coefficient of determination (R^2) of the ANN models is 0.903. The root-mean-square-error (RMSE) for the best ANN is obtained at 1.3723, mean average error (MAE) of 0.650, and a standard error of prediction (SEP) is 0.57259489.

4. Conclusion

Biodiesel production as developing alternative fuels is intriguing. The use of *C. icaco* in biodiesel production reduces the cost of biodiesel. It is advantageous because *C. icaco* is inexpensive and widely available. We have shown potential for future commercialisation of biodiesel production from *C. icaco* using calcined PSA as a catalyst(Mishra & Goswami, 2018)(Mishra & Goswami, 2018)(Mishra & Goswami, 2018)(Mishra & Goswami, 2018)(Mishra & Goswami, 2018)(Mishra & Goswami, 2018)(Mishra & Goswami, 2018)(Mishra & Goswami, 2018)(Mishra & Goswami, 2018)(Mishra & Goswami, 2018)(Mishra & Goswami, 2018). From our study, the oil yield of the crops was suitable for commercial biodiesel production of *C. icaco* (51.90%). The activities of the catalyst varied based on their pore sizes and hydrolytic stability. SEM images of the catalyst showed that the calcined form of the catalyst had a larger surface area than the raw and acid-activated. The reusability of the catalyst for continuous reaction runs was studied under the same operation conditions, and it was observed that the biofuel yield was still high after five runs. The ANN environment from MATLAB proved to be a beneficial tool for correlation and simulation. ANN offered an accurate analysis of complicated issues. As a result, it has been demonstrated that ANN may be used to forecast the performance of *C. icaco* seed oil as

a potential oil for biodiesel. In this approach, instead of expensive and time-consuming experimental investigations, it would be able to perform time- and cost-effective experiments.

5. References

Ajiwe, V., Mbonu, S. & Enukorah, E. (2006). *Solar Energy society of Nigeria*, 247-252.

Ambat, I., Srivastava, V. & Sillanpää, M. (2018). *Renewable and sustainable energy reviews* **90**, 356-369.

Arulsudar, N., Subramanian, N. & Murthy, R. (2005). *J Pharm Pharm Sci* **8**, 243-258.

Ayoola, A., Hymore, F., Omonhinmin, C., Babalola, P., Fayomi, O., Olawole, O., Olawepo, A. & Babalola, A. (2020). *Chemical Data Collections* **28**, 100478.

Babalola, P. O., Bolu, C. A., Inegbenebor, A. O. & Kilanko, O. (2018). *IOP Conference Series: Materials Science and Engineering*, p. 012063. IOP Publishing.

Balik, L., Horalek, J., Sobeslav, V. & Hornig, O. (2014). *2014 5th International Conference on Data Communication Networking (DCNET)*, pp. 1-7. IEEE.

Barabás, I. & Todoruţ, I.-A. (2011). *Biodiesel-quality, emissions and by-products*, 3-28.

Berthiaume, D. & Tremblay, A. (2006). *Oleotek Inc., NRCan project CO414 CETC-327*.

Bravo-Moncayo, L., Lucio-Naranjo, J., Chávez, M., Pavón-García, I. & Garzón, C. (2019). *Applied Acoustics* **156**, 262-270.

Calais, P. & Clark, A. (2004). *Murdoch University and Western Australian Renewable Fuels Association: Murdoch University, Western Australia*.

Dash, S. & Lingfa, P. (2018). *IOP Conference Series: Materials Science and Engineering*, p. 012006. IOP Publishing.

de Aguiar, T. M., Luo, R., Mello, A. A., Azevedo-Meleiro, C. H., Sabaa-Srur, A. U. O., Tran, K. & Smith, R. E. (2017). *Journal of Regulatory Science*, 15-28.

Desai, K. M., Survase, S. A., Saudagar, P. S., Lele, S. & Singhal, R. S. (2008). *Biochemical Engineering Journal* **41**, 266-273.

Ewim, D. R. E., Okwu, M. O., Onyiriuka, E. J., Abiodun, A. S., Abolarin, S. M. & Kaood, A. (2022). *Engineering and Applied Science Research* **49**, 444-458.

Ezekwe, C. & Ajiwe, V. (2011). *Journal of Anachem* **5**, 1016-1028.

Feitosa, E. A., Xavier, H. S. & Randau, K. P. (2012). *Revista Brasileira de Farmacognosia* **22**, 1181-1186.

Ghazali, W. N. M. W., Mamat, R., Masjuki, H. H. & Najafi, G. (2015). *Renewable and Sustainable Energy Reviews* **51**, 585-602.

Gholami, A., Pourfayaz, F. & Maleki, A. (2020). *Frontiers in Energy Research*, 144.

Giakoumis, E. G. & Sarakatsanis, C. K. (2019). *Energies* **12**, 422.

Hamad, K., Khalil, M. A. & Shanableh, A. (2017). *Transportation Research Part D: Transport and Environment* **53**, 161-177.

Jaichandar, S. & Annamalai, K. (2011). *Journal of Sustainable Energy & Environment* **2**, 71-75.

Juliana, A. O. & Egbulefu, A. V. I. (2015). *Journal of Energy and Natural Resources* **4**, 40.

Kara, K., Ouanji, F., El Mahi, M., Kacimi, M. & Mahfoud, Z. (2019). *Biofuels*.

Khudsange, C. R. & Wasewar, K. L. (2017). *International Journal of Chemical Reactor Engineering* **15**.

Knothe, G. & Steidley, K. R. (2005). *Fuel* **84**, 1059-1065.

Knothe, G. & Steidley, K. R. (2018). *Fuel Processing Technology* **177**, 75-80.

Kostić, M. D., Veličković, A. V., Joković, N. M., Stamenković, O. S. & Veljković, V. B. (2016). *Waste Management* **48**, 619-629.

Krenker, A., Bešter, J. & Kos, A. (2011). *Artificial Neural Networks: Methodological Advances and Biomedical Applications. InTech*, 1-18.

Laskar, I. B., Rajkumari, K., Gupta, R., Chatterjee, S., Paul, B. & Rokhum, L. (2018). *RSC Adv* **8**, 20131-20142.

Maran, J. P., Sivakumar, V., Thirugnanasambandham, K. & Sridhar, R. (2013). *Alexandria Engineering Journal* **52**, 507-516.

Mishra, V. K. & Goswami, R. (2018). *Biofuels* **9**, 273-289.

Ogbu, I. & Ajiwe, V. (2016). *Renewable Energy* **96**, 203-208.

Ogbu, I. M., Ajiwe, V. I. E. & Okoli, C. P. (2018). *BioEnergy Research* **11**, 772-783.

Okonkwo, C. P., Ajiwe, V. I. E., Obiadi, M. C. & Okwu, M. (2021). *American Journal of Applied Chemistry* **9**, 154-163.

Okwu, M. O., Chukwu, V. U. & Oguoma, O. (2019). *International Work-Conference on Artificial Neural Networks*, pp. 539-554. Springer.

Pikula, K., Zakharenko, A., Stratidakis, A., Razgonova, M., Nosyrev, A., Mezhuev, Y., Tsatsakis, A. & Golokhvast, K. (2020). *Green Chemistry Letters and Reviews* **13**, 275-294.

Ramirez, M. V. (2021). *Revista Colombiana de Ciencias Pecuarias* **34**, 155-160.

Sanjay, B. (2013). *Research Journal of Chemical Sciences* _____ *ISSN* **2231**, 606X.

Satya Lakshmi, S. B. A. V., Niju, S., Khadhar Mohamed, M. S. B. & Narayanan, A. (2020). *Energy Sources, Part A: Recovery, Utilization, and Environmental Effects*, 1-16.

Shahid, E. M. & Jamal, Y. (2011). *Renewable and Sustainable Energy Reviews* **15**, 4732-4745.

Singh, D., Sharma, D., Soni, S., Sharma, S., Sharma, P. K. & Jhalani, A. (2020). *Fuel* **262**, 116553.

Steinbach, L. & Altinsoy, M. E. (2019). *Applied Acoustics* **145**, 149-158.

Thiruvengadaravi, K., Nandagopal, J., Bala, V. S. S., Kirupha, S. D., Vijayalakshmi, P. & Sivanesan, S. (2009). *Indian Journal of science and Technology* **2**, 20-24.

Verma, D., Raj, J., Pal, A. & Jain, M. (2016). *Journal of Scientific and Innovative Research* **5**, 51-58.

Wang, L., Dong, X., Jiang, H., Li, G. & Zhang, M. (2014). *Bioresource technology* **158**, 392-395.

White, P. A., Araújo, J. M., Cercato, L. M., Souza, L. A., Barbosa, A. P. O., Quintans-Junior, L. J., Machado, U. F., Camargo, E. A., Brito, L. C. & Santos, M. R. V. (2016). *Journal of medicinal food* **19**, 155-160.